CONSTRAIN THE EVOLUTION OF MARTIAN ATMOSPHERE THROUGH ANALYSIS OF THE IMPACT EJECTA. Zac Yung-Chun Liu[1] and Manoochehr Shirzaei[1], [1]School of Earth and Space Exploration, Arizona State University, Tempe, AZ, USA 85287 (zacycliu@asu.edu).

Introduction: The evolution of the atmosphere of Mars is one of the most engaging questions in planetary science. Whether or not Mars may once have had a warmer and wetter past, is likely linked to the partial density and pressure of greenhouse gases in the atmosphere, in particular, carbon dioxide. While much work has focused on the plausibility of a young and dense atmosphere, the early Mars atmospheric properties, such as its density and pressure, as well as their spatiotemporal variations remain poorly constrained.

The analysis of bomb sag produced by explosive volcanic eruption infers that the atmospheric density exceeded 0.4 kg/m^3 at the time of eruption [1], much higher than the present atmospheric density (0.02 kg/m^3). Another study using small ancient craters to infer the atmospheric pressure about 3.6 Gyr ago [2], shows that the pressure is not high enough (~0.9-1.9 bar) to sustain surface liquids in the condition of faint young sun [3]. So far, previous estimates have only provided an snapshot of the atmospheric properties (e.g. density and/or pressure) in certain locations on Mars. A more recent study suggests that punctuated volcanic activity can lead to temporary warm climate [4], consistent with evidence for transient liquid water on Martian surface. However, constraints on the spatiotemporal evolution of the Martian atmospheric properties remain elusive. The estimates of atmospheric properties variations through time and space are required to understand the interplay of climate and surface geology.

To better constrain Mars atmospheric properties as well as their spatiotemporal variations, this research work establishes links between distribution of the impact ejecta, age of the impact and the local Martian atmosphere. Following an impact event, a significant volume of material is ejected and falling debris surrounds the crater. Aerodynamics rule governs the flight path and distribution of these ejecta, which indicates that the atmospheric properties play a key role in determining the spatial distribution of the ballistic particles. Given the radial distance of the ejecta from crater, an inverse aerodynamic modeling approach can be employed to estimate the local atmospheric drags and density as well as the lift forces at the time of impact. Moreover, having the spatial distribution of the craters and their ages, it is possible to resolve spatiotemporal variations of the atmospheric properties. These observations and estimations allow us to shade light on several debated questions such as how Mars evolved into the planet that we know today and whether it was once habitable.

Datasets: Robbins and Hynek (2012) [5,6] recently establish a new global catalog of Martian craters statistically complete to diameters D ≥ 1 km, which comprises 384,343 craters. In this database, the ejecta morphologic and morphometric data of the chosen craters are used to facilitate mapping the ejecta outline and estimate the ballistic ejecta distance to the crater as the inputs to the inverse aerodynamic model. Additionally, Robbins et al. (2013) [7] uses their new global crater database to estimate the age of 78 craters with diameters D ≥ 150 km based on the crater densities as well as isochron fits technique.

Mangold et al. (2012) [8] examine the degradation of impact craters in two highlands of Mars, north of Hellas Planitia, and south of Margaritifer Terra, which yield the relative chronology of these craters, based on the degradation level. Among Mangold crater age datasets, 62 craters with preserved ejecta blankets are used for our mapping. Table 1 summarizes the available crater age data from [7] and [8].

Table 1. Summary of available 140 crater age data

Epoch	Time (Ga) Hartmann (2005)	#Craters Robbins (2013)	#Craters Mangold(2012)
Noachian	4.5 - 3.74	77	2
Hesperian	3.74 - 3.46	0	30
Amazonian	< 3.46	1	30

The high-resolution Mars imagery we used to map the outlines of impact ejecta blankets and measure the ejecta distance to the crater include: (1) High Resolution Imaging System (HiRISE) images (25-50 cm/pixel resolution) [9], (2) Thermal Emission Imaging System (THEMIS) images (100 m/ pixel resolution) [10], (3) Context Camera (CTX) images (10-40 m/ pixel) [11]. Mars Orbiter Laser Altimeter (MOLA) gridded data at 463 m/pixel [12] and HiRISE DEM [9] are used to extract topographic information for the surveyed craters and identify possible impact ejecta blankets.

Methodology: *Ejecta distance estimation through mapping.* 78 large size craters (D ≥ 150 km) from the study of [7] and 62 medium/ small size craters (20 km ≤ D ≤ 180 km) from the database of [8] are carefully examined to identify crater ejecta blankets in THEMIS, CTX, and HiRISE images, assisting by topographic data of MOLA and HiRISE DEM. Fig. 1 is an example of our mapping strategies. First, we compare THEMIS, HiRISE and CTX images with MOLA DEM to carefully identify the ejecta blanket and map the ejecta outline (Fig. 1). Then, draw a series of lines starting from the center of crater to the outmost layers of ejecta blanket (Fig. 1). The line length will be an input to our inverse aerodynamic model. In order to optimize the best resolution of our inverse model we will

obtain 50+ lines (ejecta distance to the crater) for each target crater.

Inverse aerodynamic modeling. The calculation and simulation of sports balls trajectory have been well-established in the field of aerodynamics [13,14]. The trajectory of a golf ball can be explained using the following differential equation of motion [14]:

$$\frac{d^2x}{d^2t} = -\frac{\rho s}{2m}\left[\left(\frac{dx}{dt}\right)^2 + \left(\frac{dy}{dt}\right)^2\right] \times [C_d cos\beta + C_l sin\beta]$$

$$\frac{d^2y}{d^2t} = \frac{\rho s}{2m}\left[\left(\frac{dx}{dt}\right)^2 + \left(\frac{dy}{dt}\right)^2\right] \times [C_l cos\beta + C_d sin\beta] - g$$

$$\beta = tan^{-1}\left(\frac{dx}{dt} / \frac{dy}{dt}\right)$$

where x and y are measured in horizontal and vertical directions, t is time, ρ is the air density, s is the area of the ball, m is the mass of the ball, g is gravitational constant, C_d is atmospheric drag coefficient, C_l is the lift coefficient and β is the inclination angle.

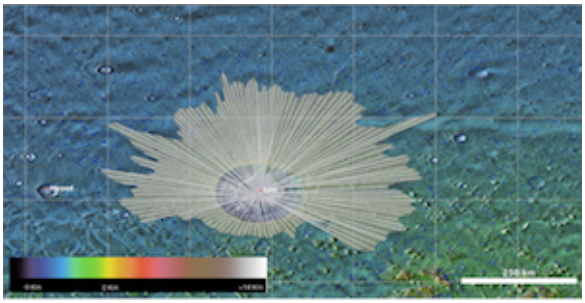

Fig. 1. An example of the mapping strategies(Lyot crater).

In analogy with golf, the impact crater ejecta resemble the ball, which following the impact is hit and thrown out of the crater. Similar to the golf ball, the ejecta trajectory is determined by the size of the impact, size and shape of the debris and the atmospheric properties. Availability of a database containing the distribution of the ejecta as well as the age of the impact crater allows inverting system of equations to estimate atmospheric properties as a function of time and location. The parameters used in the aerodynamic models are summarized in Table 2.

Table 2. Parameters used in aerodynamic modeling

Parameters	Definition	Values
x	Ejecta distance to crater	Measured
d	Density of ejecta material	2900 Kg/m^3
s	Surface area of ejecta block	s = 4πr^2
r	Radius of ejecta block	Estimated
m	Mass of ejecta block	m = d×3/4×πr^3
C_d	Atmospheric drag coef.	0-1.0
C_l	Atmospheric lift coef.	0-1.0
β	Ejection inclination	30°-70°
g	Gravitational acceleration	3.711 m/s^2

We incorporate reasonable value ranges for inclination angle, atmospheric drag and lift coefficients in the model. The measured ejecta distances to crater also contain uncertainty range. In order to better solve the second-order differential trajectory equations by inputting estimated parameters and obtain the best solution of atmospheric density, the optimization techniques are adopted. The random search computing techniques have successfully provided great solutions for inverse models [15]. In this study, we adopt the genetic algorithm (GA) to resolve the inverse model composed of the differential equations.

Validation of inverse aerodynamic model: A recent impact event occurred between July 2012 and May 2012, which has been observed by HiRISE images. In order to validate our methodology and optimization technique, we map the ejecta of the 2012 impact event carefully and measure the ejecta distance to crater center. We obtained 55 measurements of ejecta distance and azimuth of measured line (Fig. 2). The crater diameter is approximately 30 m. The longest ejecta distance mapped is 2.5 km while the shortest one is 0.4 km.

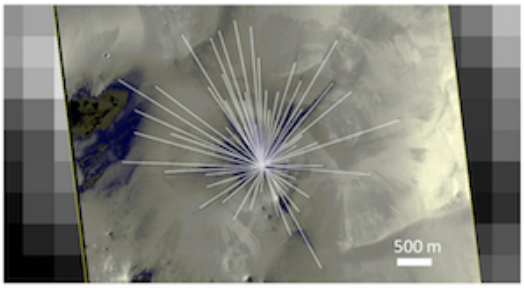

Fig. 2. Ejecta mapping of 2012 impact crater.

The best solution found in our inversion predict surface atmospheric density of 0.0216 ± 0.003 kg/m^3, which is in a good agreement with the recent measurements, surface density of 0.02 kg/m^3, and approves the feasibility of our methodology and inversion technique. Moreover, using the concept of error propagation [16], we find that a 20% error in measuring the ejecta distances may cause only a 0.2% error in the estimated atmospheric density. These promising preliminary results indicate continued work on the chosen (+100) crater ejecta will generate solid and convincing results and allow us to better infer the Martian atmospheric evolution and spatiotemporal variations on air density, which will be appropriate for the discussions in the Special Session on Tracing the Evolution of the Ancient Martian Atmosphere and Climate.

References: [1] Manga M. et al. (2012) *GRL, 39,* L01202. [2] Kite E.S. et al. (2014) *Nature Geo., 7,* 335-339. [3] Gaidos C.G. (2000) *GRL, 27*,501-503. [4] Halevy I. and Head J.W. (2014) *Nature Geos. 2293.* [5] Robbins S.J. and Hynek B.M. (2012a) *JGR, 117*, E05004. [6] Robbins S.J. and Hynek B.M. (2012b) *JGR, 117*, E6. [7] Robbins S.J. et al. (2013) *Icarus*, *225*(1), 173-184. [8] Mangold et al. (2012) *JGR, 117*, E4. [9] McEwen A.S. et al. (2007) *JGR, 112*, E05S02. [10] Christensen P.R. et al. (2003) *Science, 300*, 2056-2061. [11] Malin M.C. et al. (2007) *JGR, 112*, E05S04. [12] Smith D.E. et al. (1999) *Science*, 284(5419), 1495–1503. [13] Davies L. (1949) *J. of App. Physics*, 20(9), 821-828. [14] Mehta R.D. (1985) *Ann. Review of Fluid Mechanics*, 17, 151-189. [15] Shirzaei M. and Walter T.R. (2009) *JGR*, 114(B10). [16] Mikhail, E. M. (1976). *Observations and least squares*, New York, IEP.